Title

Toward optimization of in vivo super-resolution ultrasound imaging using size-selected microbubble contrast agents

Journal

Medical Physics, 44(12)

ISSN

0094-2405

Authors

Ghosh, Debabrata
Xiong, Fangyuan
Sirsi, Shashank R
et al.

Publication Date

2017-12-01

DOI

10.1002/mp.12606

Peer reviewed

Toward optimization of *in vivo* super-resolution ultrasound imaging using size-selected microbubble contrast agents

Debabrata Ghosh
Department of Bioengineering, University of Texas at Dallas, Richardson, TX 75080, USA
Department of Radiology, University of Texas Southwestern Medical Center, Dallas, TX 75390, USA

Fangyuan Xiong
Department of Bioengineering, University of Texas at Dallas, Richardson, TX 75080, USA
Department of Medical Ultrasound, Huazhong University of Science and Technology, Wuhan, China

Shashank R. Sirsi
Department of Bioengineering, University of Texas at Dallas, Richardson, TX 75080, USA
Department of Radiology, University of Texas Southwestern Medical Center, Dallas, TX 75390, USA

Philip W. Shaul
Department of Pediatrics, Center for Pulmonary and Vascular Biology, University of Texas Southwestern Medical Center, Dallas, TX 75390, USA

Robert F. Mattrey
Department of Radiology, University of Texas Southwestern Medical Center, Dallas, TX 75390, USA

Kenneth Hoyt[a)]
Department of Bioengineering, University of Texas at Dallas, Richardson, TX 75080, USA
Department of Radiology, University of Texas Southwestern Medical Center, Dallas, TX 75390, USA

(Received 13 April 2017; revised 9 August 2017; accepted for publication 30 August 2017; published 27 October 2017)

Purpose: Microvascular processes play key roles in many diseases including diabetes. Improved understanding of the microvascular changes involved in disease development could offer crucial insight into the relationship of these changes to disease pathogenesis. Super-resolution ultrasound (SR-US) imaging has showed the potential to visualize microvascular detail down to the capillary level (i.e., subwavelength resolution), but optimization is still necessary. The purpose of this study was to investigate *in vivo* SR-US imaging of skeletal muscle microvascularity using microbubble (MB) contrast agents of various size and concentration while evaluating different ultrasound (US) system level parameters such as imaging frame rate and image acquisition length.
Methods: An US system equipped with a linear array transducer was used in a harmonic imaging mode at low transmit power. C57BL/6J mice fed a normal diet were used in this study. An assortment of size-selected MB contrast agents (1–2 μm, 3–4 μm, and 5–8 μm in diameter) were slowly infused in the tail vein at various doses (1.25×10^7, 2.5×10^7, or 5×10^7 MBs). US image data were collected before MB injection and thereafter for 10 min at 30 frames per s (fps). The US transducer was fixed throughout and between each imaging period to help capture microvascular patterns along the same image plane. An adaptive SR-US image processing technique was implemented using custom Matlab software.
Results: Experimental findings illustrate the use of larger MB results in better SR-US images in terms of skeletal muscle microvascular detail. A dose of 2.5×10^7 MBs resulted in SR-US images with optimal spatial resolution. An US imaging rate of at least 20 fps and image acquisition length of at least 8 min also resulted in SR-US images with pronounced microvascular detail.
Conclusions: This study indicates that MB size and dose and US system imaging rate and data acquisition length have significant impact on the quality of *in vivo* SR-US images of skeletal muscle microvascularity. [https://doi.org/10.1002/mp.12606]

Key words: contrast-enhanced ultrasound, diabetes, microbubbles, super-resolution ultrasound

1. INTRODUCTION

Microvascular events are known to play important roles in many diseases such as diabetes. For instance, attenuation in skeletal muscle microvascular response to insulin leads to impaired microvascular recruitment and plays a critical role in the progression of type 2 diabetes.[1] Improved understanding of the microvascular changes involved in disease development could offer crucial insight into the relationship of these changes with the pathology, and thus may allow development of novel and more effective therapeutic strategies.[2]

Despite intensive efforts, monitoring changes in the microvasculature remains a challenging task, mainly due to

the resolution limitation of traditional medical imaging modalities. Considering the different noninvasive imaging modalities that populate most hospitals, X-ray computed tomography (CT) has a blood vessel detection limit of 400 μm,[3] and magnetic resonance imaging has a limit of about 300 μm,[4] which is comparable to ultrasound (US) at clinical imaging frequencies.[5] In clinical imaging, US has been considered the best alternative to the other modalities due to its compact size, nonionizing radiation, low cost, and relatively faster image acquisition. While the use of microbubble (MB) contrast agent during US imaging (termed dynamic contrast-enhanced US, DCE-US) improves the detection of small blood vessels,[6,7] it still lacks the spatial resolution necessary to differentiate vessels at the capillary level where a bulk of the skeletal muscle microvascular recruitment manifests.[8] While acoustic angiography is a promising US imaging method that exhibits a spatial resolution of about 150 μm,[9] frequency-dependent attenuation constrains the applicability of this technique to relatively shallow tissue depths.[10]

Super-resolution US (SR-US) is a new imaging method that has shown promise for providing image spatial resolutions greater than the diffraction limit of the US system (< 50 μm).[11,12] In approach, SR-US relies on the precise localization of individual microbubble (MB) contrast agents that have been injected and are flowing intravascularly.[13] These contrast agents are excellent point scatterers and detection has been simplified with the use of dedicated US imaging techniques that monopolize a MBs nonlinear behavior in an US field.[14] The subsequent use of spatiotemporal filtering allows additional suppression of any tissue and background signal to improve automated MB localization.[15,16] In the last few years, the potential of SR-US imaging has been demonstrated for several diverse small animal applications ranging from microvascular imaging of renal[17] and brain[16] tissue perfusion to tumor angiogenesis.[18,19]

A fundamental question remains as how to optimize SR-US imaging for widespread preclinical application. Christensen–Jeffries et al. recorded US data at a moderate frame rate (~25 fps) and achieved dense spatial distribution after MB localizations.[20] To make the MBs spatially separable, they infused a dilute suspension of contrast media. Foiret et al. recorded US data at 300 fps for a shorter acquisition time (3 min after injection of 3×10^7 MBs), claiming a higher frame rate helps maximize the correlation between adjacent frames, which was critical for their motion correction strategy.[17] Conversely, Errico et al. used ultrafast frame rates (500 fps) and a slightly shorter acquisition time (150 s for brain cortex, 10 min for whole-brain studies) to obtain SR-US images of tissue microvascularity after MB administration (1.3×10^7 MBs).[16,19] In this article, we investigate the *in vivo* performance of SR-US imaging of skeletal muscle microvascularity using (a) various size-selected MBs, (b) different MB concentrations, (c) different US imaging frame rates, and (d) range of image acquisition times in order to help optimize SR-US image quality. We note that the impact of MB size on SR-US imaging has not been studied *in vivo* to date. Because MB size is intimately related to acoustic backscatter and *in vivo* circulation persistence, understanding the role of MB size on SR-US imaging is crucial.

2. MATERIALS AND METHODS

Animal experiments were reviewed and approved by the Institutional Animal Care and Use Committee (IACUC) at the University of Texas at Dallas. Healthy six-week-old C57BL/6J mice (Charles River Laboratories, Wilmington, MA, USA) fed a normal diet were used in our study. The fur was removed from the left proximal hindlimb adductor muscle group of each animal. Image data were acquired using a clinical US scanner (Acuson Sequoia 512; Siemens Healthcare, Mountain View, CA, USA) equipped with a 15L8-S linear array transducer. The US transducer was fixed throughout each imaging period to help capture microvascular patterns along the same image plane. A contrast pulse sequencing (CPS) imaging mode (transmit/receive at 14 MHz) was used at a low acoustic output (mechanical index, MI = 0.2) to improve MB-to-tissue specificity. These DCE-US data were collected at a frame rate of 30 fps and depth of 20 mm while using a single transit focus located at 10 mm. The scan-converted DCE-US image grid size was 0.06 mm in the axial and lateral dimensions. US system settings remained fixed throughout the experiments. During all imaging sessions, animals were placed on a heating pad to maintain core temperature and controlled with 2%–3% isoflurane anesthesia (V3000PK; Parkland Scientific, Coral Springs, FL, USA).

Size-selected MBs were manufactured and purchased (1–2 μm, 3–4 μm, and 5–8 μm; Advanced Microbubble Laboratories, Boulder, CO, USA) and subsequently characterized (size and concentration) using a small particle sizer (Multisizer 3 Coulter Counter, Beckman Coulter, Brea, CA, USA). Unless otherwise noted, contrast agent suspensions of 1.25×10^7, 2.5×10^7, or 5×10^7 MBs were slowly infused (over a duration of 10 s) via a 27G winged infusion catheter (Terumo Corp, Hatagaya, Tokyo, Japan) placed in the tail vein. DCE-US image data were collected before MB injection and thereafter for 10 min. Note that MB injections were randomized for each animal, and there was a 1-h delay between any subsequent doses to allow MB clearance as confirmed by US imaging. Since our animal experiments involved nonterminal tests, all animals were returned to our vivarium after US imaging for continued housing and daily care.

Custom MATLAB software (Mathworks Inc, Natick, MA, USA) was used to implement the SR-US image processing strategy. An empirically determined threshold value was used to eliminate any low-intensity background noise from the DCE-US image sequence. The intravascular MB signal was then differentiated from skeletal muscle tissue signal using a singular value decomposition (SVD) algorithm which functions as a high-pass spatiotemporal filter.[15] The number of singular values removed from the DCE-US data was determined adaptively based on a local contrast-to-noise ratio (CNR) value as follows:

$$\mathrm{CNR} = \frac{\mu_{MB} - \mu_B}{\sigma_B} \quad (1)$$

where μ and σ denote mean and standard deviation whereby the subscripts *MB* and *B* indicate US image region-of-interest (ROIs) containing MB and background tissue signal, respectively. The singular value number that produced the highest local CNR value was then selected for signal filtering. Briefly, the adaptive SVD algorithm initiates with a threshold value of 1 (i.e., number of singular values removed = 1). This number is then incremented until the local CNR value is maximized. The adaptive SVD threshold selection process based on local CNR analysis is illustrated in Fig. 1. After the MB signal was separated from the DCE-US data, individual MBs were identified (by finding connected components) before calculation of their intensity-weighted center of mass. To make sure detected signal was coming from a single MB, low MB dilution was essential. Upon processing the entire image stack in temporal space and mapping the cumulative MB positions, a density map is the result and constitutes a SR-US image (with same grid size as DCE-US image data). Additionally, the MB count from each DCE-US image can be plotted to describe the time history of MB circulation and can be used to derive parametric measures of tissue perfusion and microvascular function. Figure 2 summarizes the image processing strategy used to produce the SR-US images. For comparative purposes, a MIP was performed along the temporal dimension of the DCE-US image sequences to describe microvascular structures using a more traditional approach.[6] Representative time-intensity curves were generated from an ROI encompassing the hindlimb adductor muscle group and derived from DCE-US data only where microvascularity was detected in the co-registered MIP or SR-US images.

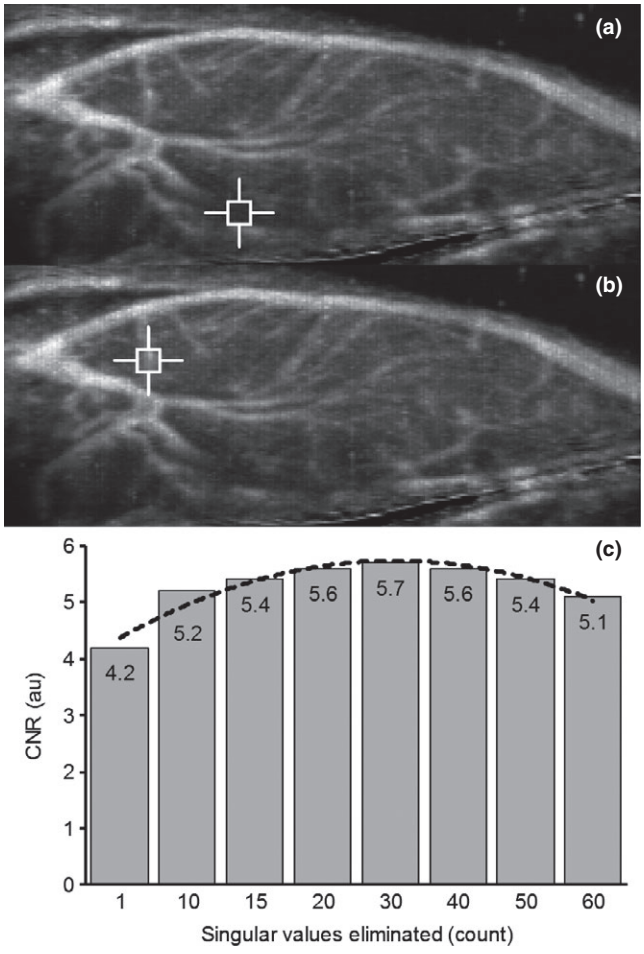

FIG. 1. Demonstration of the adaptive selection process for optimizing the number of singular values (derived from singular value decomposition of a dynamic contrast-enhanced ultrasound, DCE-US, signal) eliminated during high-pass filtering. Individual MB signals are isolated through local contrast-to-noise (CNR) value maximization. For computing local CNR, corresponding (a) background and (b) MB-containing regions (white boxes) are selected from the maximum intensity projection image after performing high-pass filtering. (c) Illustration of the CNR value changes and optimization as a function of progressive singular value elimination.

3. RESULTS

All size-selected MBs were characterized before each contrast agent injection to ensure matched dosing. Figure 3 details the size distribution for the MBs we studied, namely those with narrow diameter ranges of 1–2 μm, 3–4 μm, and 5–8 μm. A representative *in vivo* SR-US image obtained from a mouse hindlimb and using a 3- to 4-μm-sized MB is depicted in Fig. 4. A conventional maximum intensity projection (MIP) image was computed from the DCE-US sequence and presented for comparison. Note the fine skeletal muscle microvascular detail in the SR-US image that is obscured in the lower resolution MIP image. This example illustrates how the SR-US imaging approach differentiates backscattered MB from tissue signals leading to high image contrast between the microvasculature and the surrounding skeletal muscle. Microvascular structures are poorly visible in the DCE-US-based MIP image making any morphology and tissue

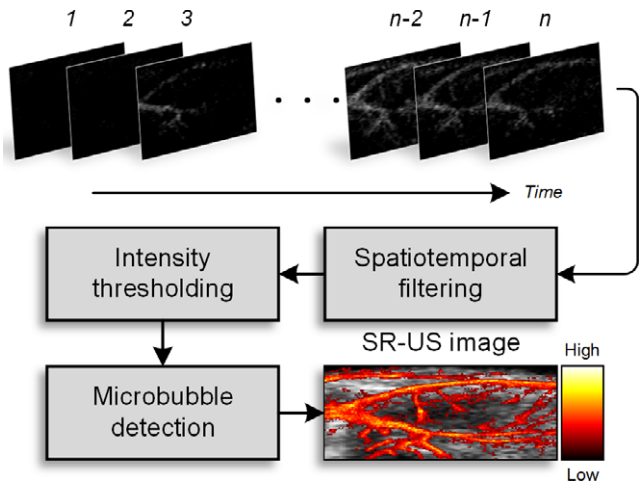

FIG. 2. Schematic diagram summarizing the major image processing steps adopted to produce a super-resolution ultrasound (SR-US) image from a length *n* time series of DCE-US. The SR-US image intensity is a quantitative spatial measure of individual MBs detected and localized during adaptive analysis of the US data. [Color figure can be viewed at wileyonlinelibrary.com]

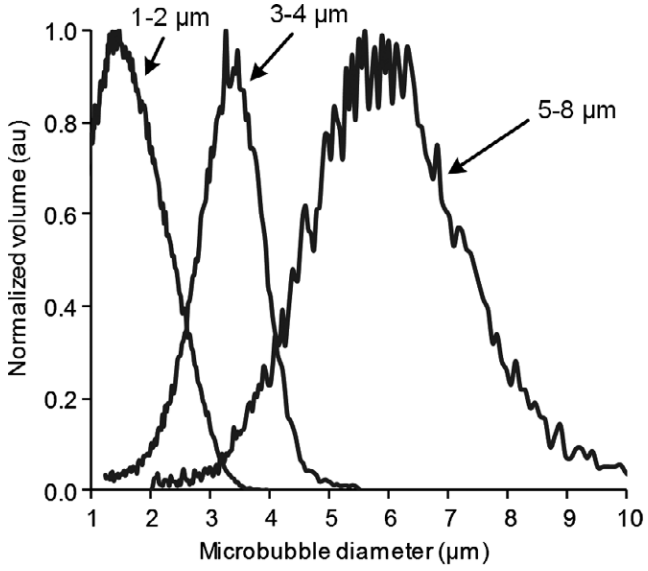

FIG. 3. Histogram plots of the different sized MBs used during the *in vivo* SR-US imaging study, namely 1–2 μm, 3–4 μm, and 5–8 μm.

perfusion analysis problematic. More specifically, Fig. 4 also shows MB profile line plots across two example vessels. The full width at half maximum (FWHM) of these plots can be used to estimate microvascular diameter and the imaging system resolution capability. Using SR-US, the diameter of the first vessel was measured to be 72.3 μm and the diameter of the second representative vessel was found to be 78.6 μm. Both are below the wavelength (and diffraction limit) of the US imaging system used (λ = 110 μm at 14 MHz). Corresponding measurements from the MIP image were 225.0 μm and 231.2 μm, respectively. These examples highlight a noticeable improvement in microvascular size estimation in skeletal muscle when using MB localization and the SR-US technique compared with the standard MIP technique.

The time history of MB circulation derived from the skeletal muscle examples in Fig. 4 is summarized in Fig. 5. The pair of time-intensity curves was derived from DCE-US data only where microvascularity was detected in the co-registered MIP or SR-US images. The MIP-derived curve is noticeably lower in amplitude and attributed to the incorporation of low-level background tissue signal or noise, which is effectively filtered out by SR-US image processing yielding a truer representation of tissue perfusion. Uniquely, SR-US imaging is founded on the ability to detect and count individual MBs flowing through the microvasculature; thus, a frame-by-frame summary can be used to produce a MB density measurement. Due to improved reduction of background noise as compared with conventional time-intensity curve-based approaches, quantitative analysis of these new time MB count curve (TMC) datasets will help minimize the variance and reproducibility issues associated with current US-based time-intensity curve analyses. Importantly, since TMC data reflect a quantitative time history of MB density, the measurement is inherently US system independent and places no restriction on the US imaging mode used with the only exception that

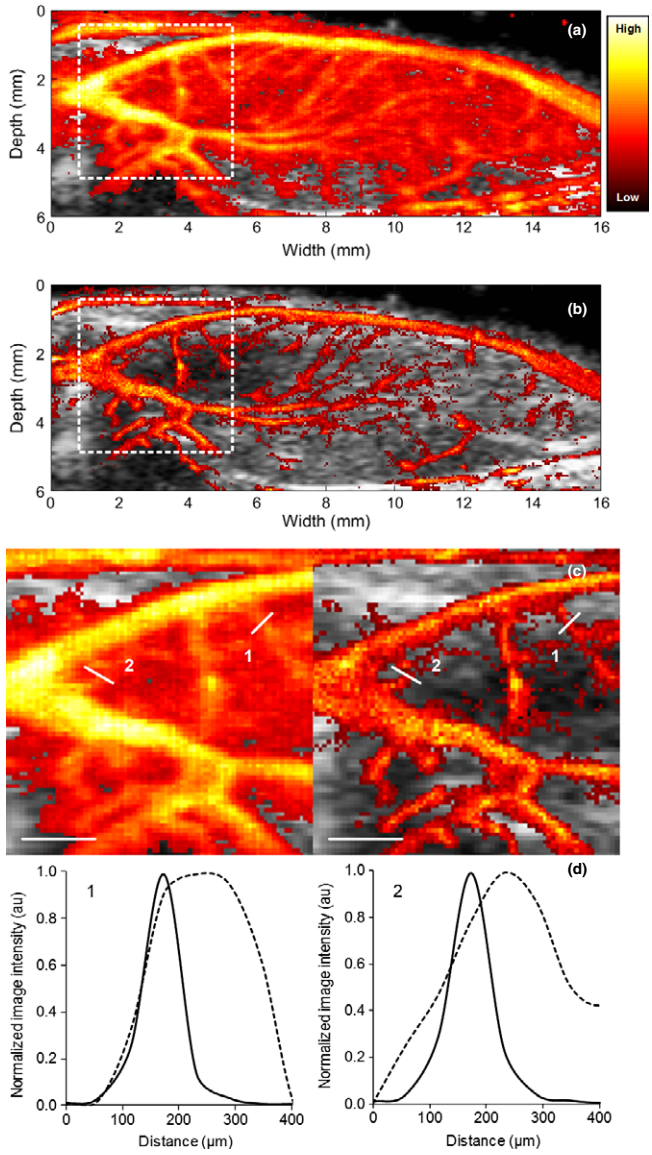

FIG. 4. Spatial maps of skeletal muscle microvascularity derived from a DCE-US data sequence and produced using either the (a) traditional maximum intensity projection (MIP) or (b) new SR-US image processing technique. From these images, enlarged areas (dashed box) in (c) illustrate the fine microvascular detail present in the SR-US image but unresolved in the corresponding MIP image. From two small vessels, (d) line profiles from both SR-US (solid lines) and MIP (dashed lines) highlight the enhanced resolution afforded by use of SR-US and a 3- to 4-μm-sized MB. [Color figure can be viewed at wileyonlinelibrary.com]

MBs can be sensitively detected and enumerated. Thus, the new TMCs may provide a greater understanding of tissue perfusion and the kinetics of MB circulation and clearance.

The impact of MB size on *in vivo* SR-US imaging in skeletal muscle is detailed in Fig. 6. Results show SR-US images obtained from the same image plane after randomized injection of 1–2 μm, 3–4 μm, or 5–8 μm sized MBs. In each case, a bolus injection containing 2.5 × 10^7 MBs was used. Data reveal that larger MBs (3–4 μm and 5–8 μm) yield better *in vivo* SR-US results in terms of image quality and skeletal microvascular network definition in the context of the experimental settings chosen in this study. Backscatter

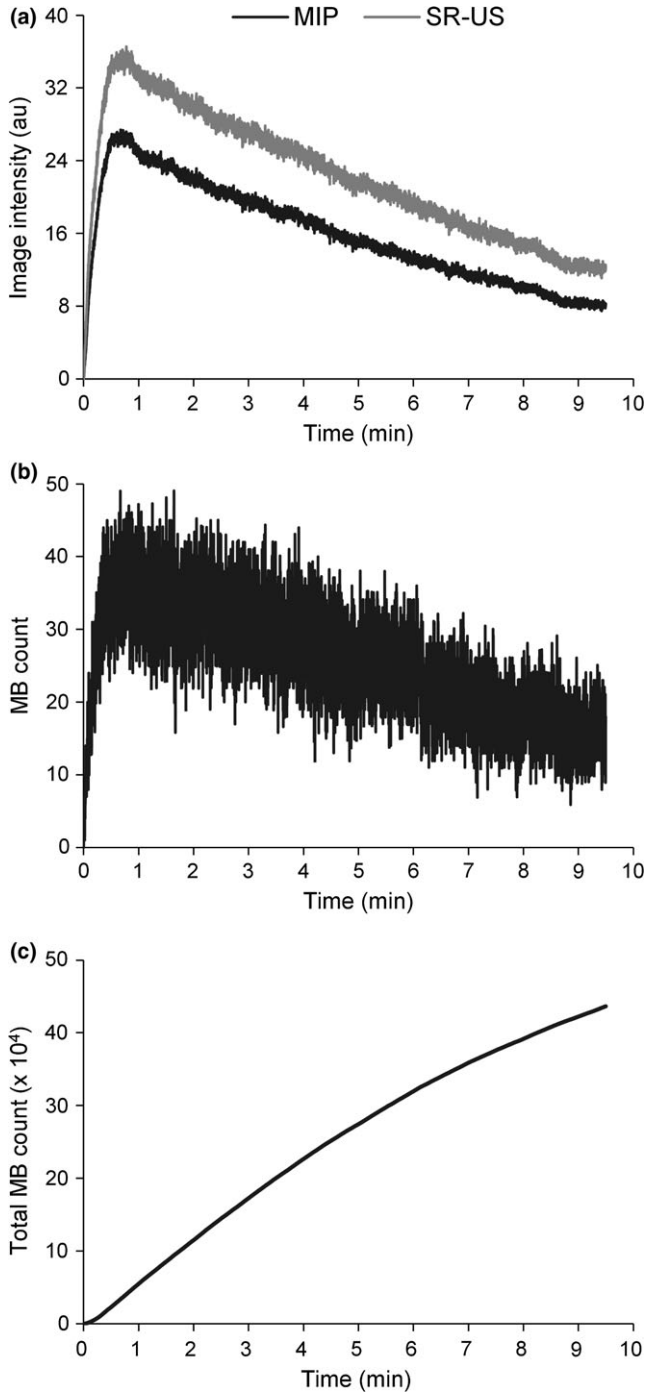

FIG. 5. Time-intensity curves obtained in skeletal muscle tissue after administration of a MB contrast agent and performing DCE-US imaging for 10 min. (a) Comparison of curves obtained from DCE-US image locations where a microvessel was detected in the co-registered MIP or SR-US images. Note the latter curve yields a higher intensity as it incorporates less background or tissue signal in the region-of-interest (ROI). Since the SR-US image processing functions by counting MBs detected in the DCE-US image sequences on a frame-by-frame basis, quantitative plots depicting both (b) MB count and (c) cumulative (or total) MB count can be produced to reflect the time history of MB flow.

signals from smaller MBs (1–2 μm) are relatively weaker during US imaging, which leads to a poorer MB detection capability during SR-US image processing. Percent microvascularity scores were calculated for each of the size-selected MB experiments ($N = 9$) as shown in Table I. Briefly, each SR-US image was binarized and a total tissue microvascularity score was reported as a % of the total image area assessed. The contrast enhancement and persistence of MBs in the circulation were analyzed from the time density plot for each size-selected MB. After selecting an ROI that encompassed the entire hindlimb abductor skeletal muscle group, a considerable difference in amplitude is observed between the time density plots obtained from use of the larger and smaller MB types. The 3- to 4-μm-sized MB population exhibited longer circulation persistence compared with 1- to 2-μm-sized MBs. Further, the 5- to 8-μm-sized MBs were observed to persist the longest in the blood stream.

Figure 7 contains SR-US images of skeletal muscle microvascularity in three different animals each administered a different sized MB (1–2 μm, 3–4 μm, or 5–8 μm) and dose:

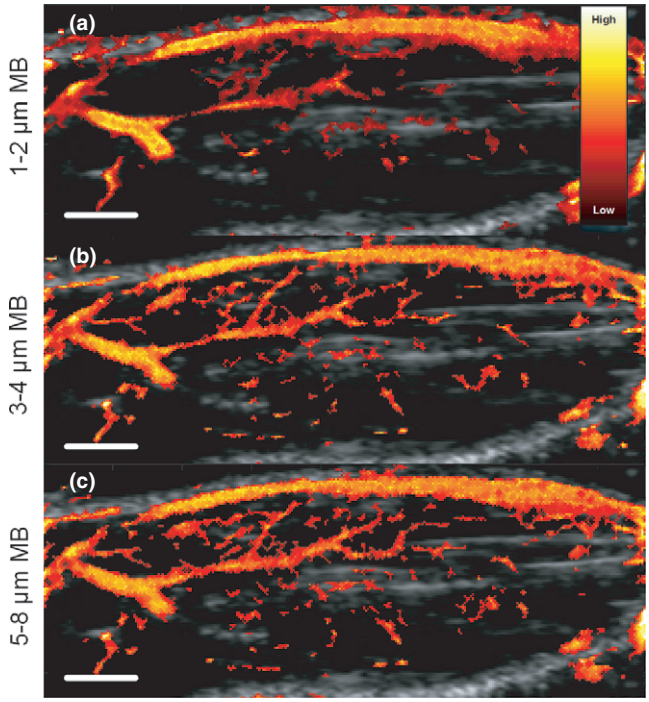

FIG. 6. *In vivo* SR-US images of skeletal muscle microvascularity obtained after bolus injections of 2.5×10^7 MBs of different size: (a) 1–2 μm, (b) 3–4 μm, or (c) 5–8 μm. The scale bar indicates 2 mm. Note all images were acquired in the same animal and tissue plane after the previous MB injection was cleared from circulation. [Color figure can be viewed at wileyonlinelibrary.com]

TABLE I. Microvascularity levels (% tissue area) calculated from *in vivo* SR-US images obtained following a bolus injection containing 2.5×10^7 MBs of different sizes, namely 1–2 μm, 3–4 μm, or 5–8 μm.

MB size	Microvascularity (% area)
1–2 μm	14.6 ± 2.8
3–4 μm	21.8 ± 2.5
5–8 μm	36.5 ± 6.7

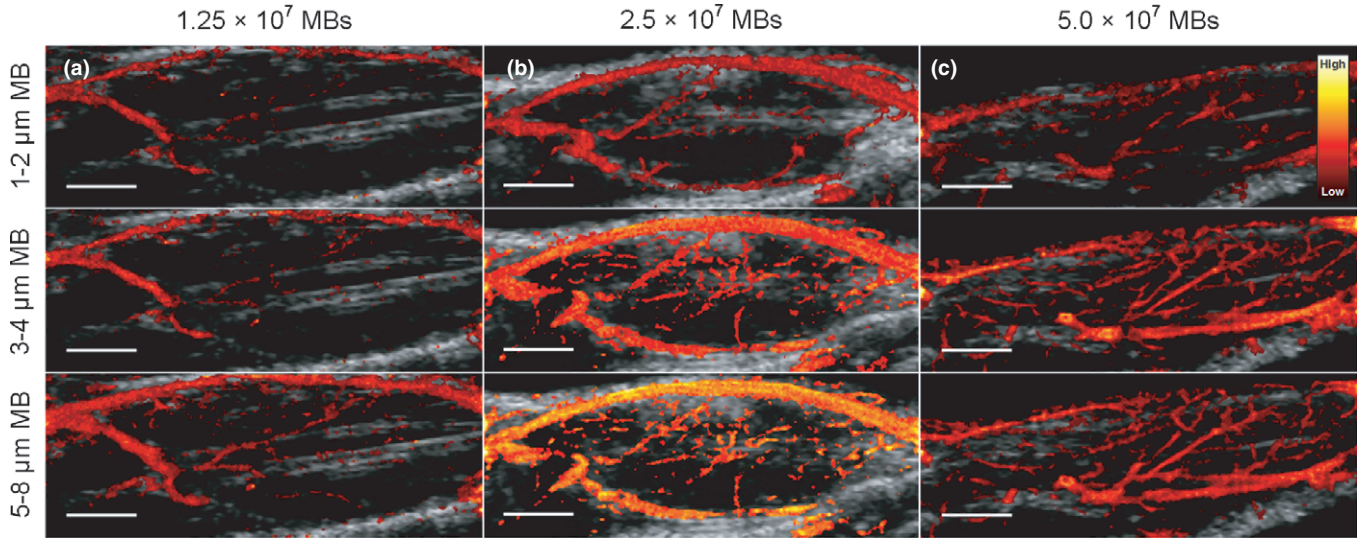

FIG. 7. *In vivo* SR-US images of skeletal muscle microvascularity obtained after bolus injections of different sized MBs: (a) 1–2 µm, (b) 3–4 µm, or (c) 5–8 µm. Image results were obtained using a range of MB doses, namely 1.25×10^7, 2.5×10^7, or 5.0×10^7 MBs per injection, top to bottom, respectively. The scale bar indicates 2 mm. [Color figure can be viewed at wileyonlinelibrary.com]

1.25×10^7 MBs, 2.5×10^7 MBs, or 5×10^7 MBs per injection. Data acquisition time (10 min) and frame rate (30 fps) were held constant throughout this experiment. The 1- to 2-µm-sized MBs produced minute DCE-US image enhancement and limited visibility of the skeletal microvasculature when a bolus injection of 1.25×10^7 MBs was administered. This limitation resulted in a low number of individual MBs detected and compromised SR-US image quality in terms of microvascular definition and structure visibility. A slight improvement was observed in microvascular detail after the use of a bolus injection containing twice as many MBs. Using the smaller MB type, the best SR-US image of skeletal muscle microvascularity was observed following an injection of 5×10^7 MBs (largest concentration evaluated). Notwithstanding, SR-US image quality was still graded relatively poor when using the 1- to 2-µm-sized MBs. Similarly, microvascularity visualization was limited in SR-US image obtained using the 3- to 4-µm-sized MBs administered at a low dose (1.25×10^7 MBs). Noticeable improvements were noted in microvascular detail when using contrast agent dose of 2.5×10^7 MBs. There was little observable change in the *in vivo* SR-US image quality when 3- to 4-µm-sized MB dose was subsequently increased (i.e., 5×10^8 MBs per injection). At low concentration (1.25×10^7 MBs), SR-US images obtained using the 5- to 8-µm-sized MBs exhibit minimum microvascular detail. As Fig. 6 further highlights, doubling the MB concentration produces *in vivo* SR-US images with considerable improvement in microvascular detail. Increasing the 5- to 8-µm-sized MB dose further had little effect on SR-US image quality. Objectively, use of the larger size-selected MB types at a moderate concentration (i.e., 2.5×10^7 MBs per injection) consistently resulted in the best SR-US images, except the 1- to 2-µm-sized MBs, for which the overall spatial resolution was graded poor.

The impact of the US imaging frame rate on SR-US image quality was investigated. Fig. 8 depicts representative *in vivo* SR-US images produced from US data acquired using size-selected MBs and a range of different frame rates (i.e., 10, 15, 20, 25, or 30 fps). Data acquisition time (10 min) and MB density (2.5×10^7 MBs per injection) were held constant throughout this experiment. Note that all US data were collected at 30 fps and lower imaging rates were achieved by image sequence down sampling before SR-US image processing. Using 1- to 2-µm-sized MBs, changes in the US imaging frame rate produced minimal changes in SR-US image quality. Consequently, very little of the skeletal muscle microvasculature is observed regardless of frame rate. Use of the 3- to 4-µm-sized MBs revealed that decreasing the US imaging frame rate resulted in a decrease in SR-US image quality in terms of microvascular detail. The greatest detail was noted when using the higher imaging frame rate (i.e., 20–30 fps). The use of a lower US imaging frame rate compromised SR-US image quality by degrading spatial resolution and exhibition of little microvascular detail. US imaging of the 5- to 8-µm-sized MBs using a varying frame rate produced similar SR-US results. Table II highlights the quantitative comparison (using % microvascularity scores) between the various SR-US imaging frame rates.

The impact of US image acquisition length (i.e., 4, 6, 8, or 10 min) on SR-US results was also evaluated (Fig. 9). During this experiment, US imaging frame rate (30 fps) and MB concentration (2.5×10^7 MBs per injection) were held constant. Note that all US data were collected for 10 min after MB injection and lower image acquisition numbers were achieved by truncating this original US series before SR-US image processing. As results detail, use of the 1- to 2-µm-sized MBs yields minimal changes in the otherwise relatively poor SR-US image quality when acquisition time was

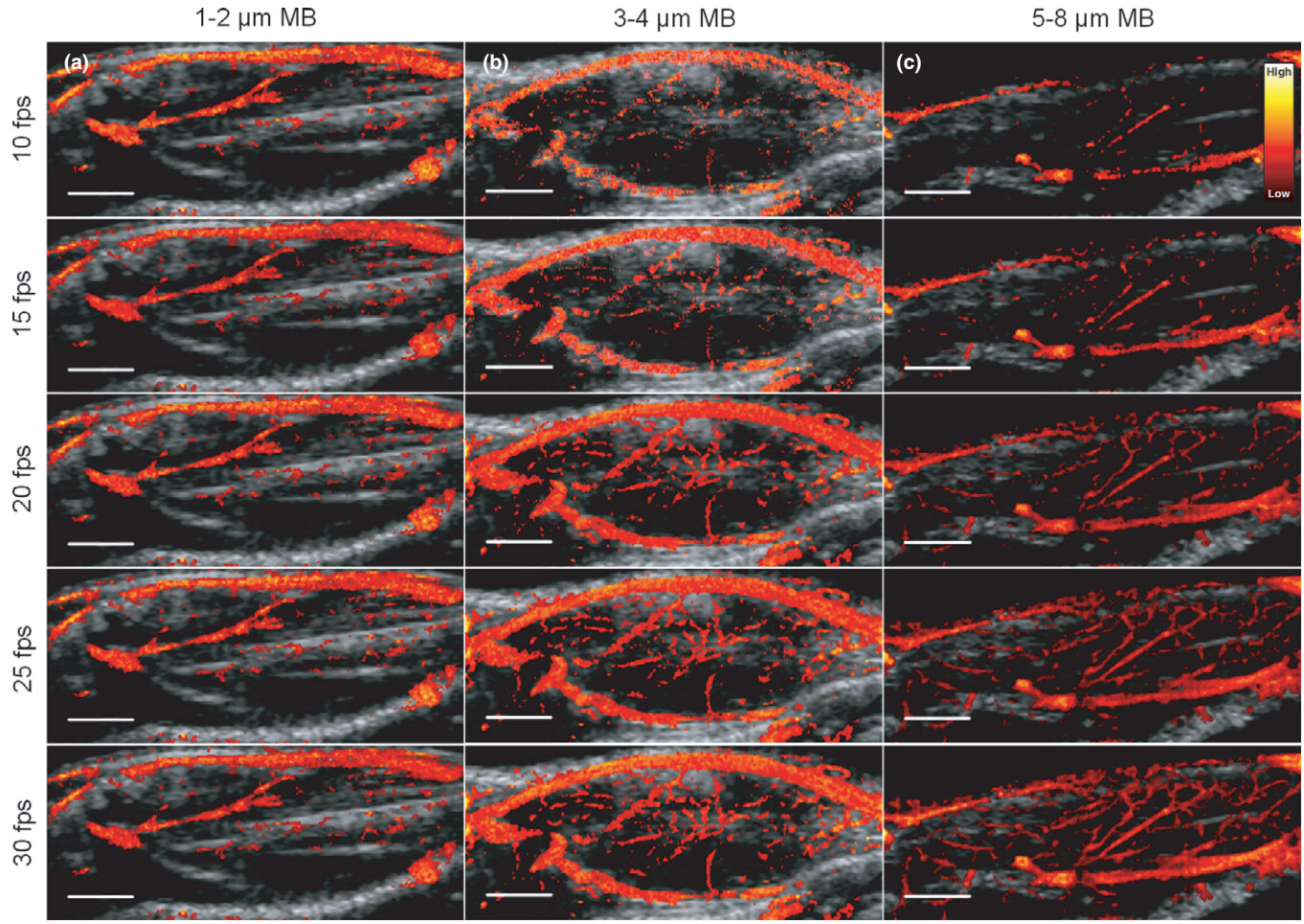

FIG. 8. *In vivo* SR-US images of skeletal muscle microvascularity obtained after bolus injections of 2.5×10^7 MBs of different size: (a) 1–2 μm, (b) 3–4 μm, or (c) 5–8 μm. Image results were obtained using a range of ultrasound (US) imaging frame rates, namely 10, 15, 20, 25, or 30 frames per s (fps), top to bottom, respectively. The scale bar indicates 2 mm. [Color figure can be viewed at wileyonlinelibrary.com]

changed from 4 to 10 min. Using 3- to 4-μm-sized MBs, noticeable changes in the resultant SR-US images, and microvascular definition contained within, were observed when acquisition time changed from 4 to 8 min. Only minor changes in SR-US image quality was noted when data acquisition time was increased beyond 8 min. Again, US imaging of the 5- to 8-μm-sized MBs using a varying image acquisition length produced comparable SR-US results. Table III highlights the quantitative comparison between the various SR-US image acquisition times.

TABLE II. Microvascularity levels calculated from *in vivo* SR-US images obtained following a bolus injection of MBs of different sizes, namely 1–2 μm, 3–4 μm, or 5–8 μm, and using a range of different US imaging system frame rates, i.e., 10, 15, 20, 25, or 30 frames per s (fps).

	Microvascularity (% area)		
Frame rate (fps)	1–2 μm	3–4 μm	5–8 μm
10	7.7 ± 0.3	10.5 ± 0.7	9.1 ± 0.2
15	8.8 ± 0.5	11.5 ± 0.8	10.1 ± 0.4
20	9.7 ± 0.7	22.5 ± 2.2	19.5 ± 0.9
25	10.3 ± 0.8	26.9 ± 0.7	23.0 ± 1.4
30	10.6 ± 0.9	28.7 ± 0.2	26.1 ± 1.0

4. DISCUSSION

In this study, we demonstrated the ability of *in vivo* SR-US imaging to depict skeletal muscle microvascular structures below the diffraction limited (subwavelength) resolution of the US imaging system used for data acquisition. All SR-US studies currently detailed in the literature report the use of either commercially available MB products or contrast agents manufactured in the laboratory using similar protocols as these products. Inherent to the formulation process, these MBs are known to be polydisperse in size distribution.[21] Given MB size has a strong influence on the intensity of the backscattered US signal, we hypothesized that the use of a more uniformly sized MB (i.e., point scatterer) could give a more consistent response from the entire MB population and improve detection during SR-US image processing.

Evaluating our adaptive SVD filter using a tissue-mimicking vascular flow phantom while ultrasound imaging of

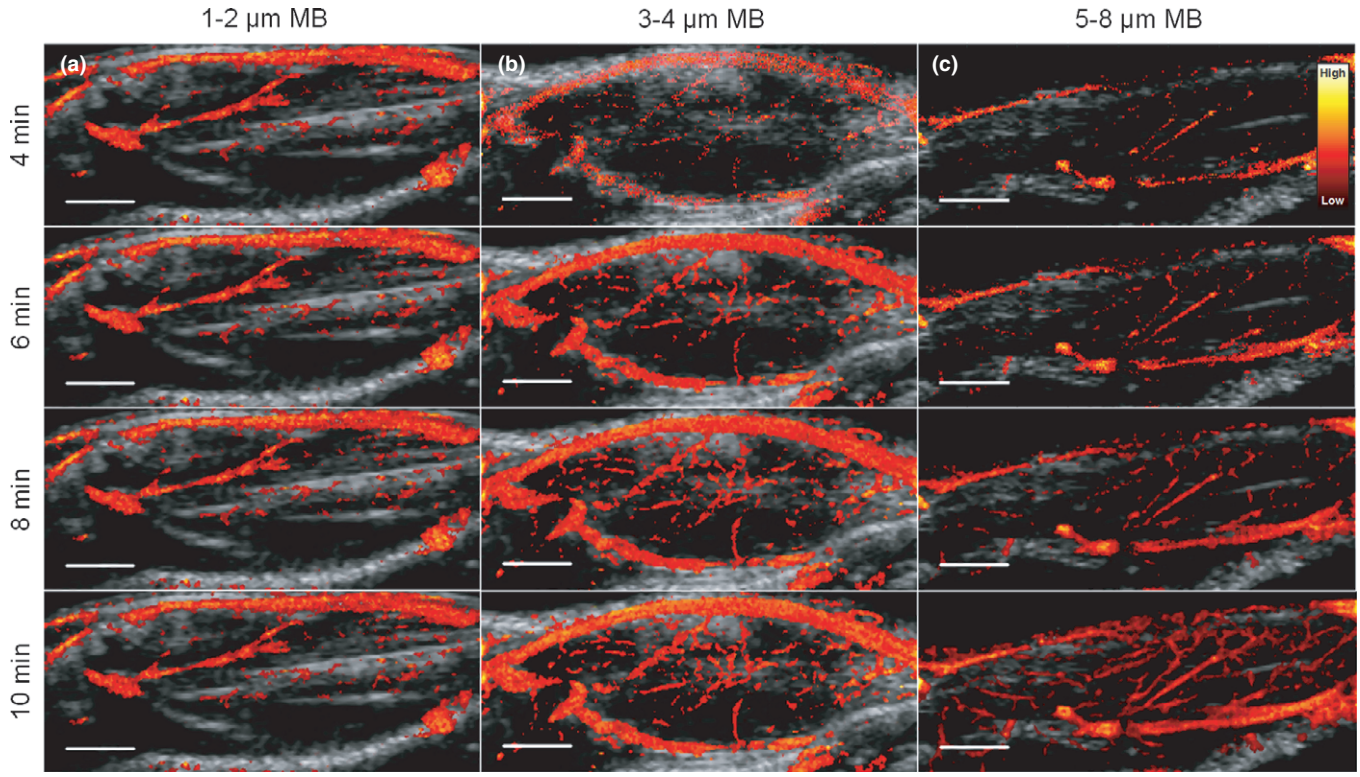

FIG. 9. *In vivo* SR-US images of skeletal muscle microvascularity obtained after bolus injections of 2.5×10^7 MBs of different size: (a) 1–2 μm, (b) 3–4 μm, or (c) 5–8 μm. Image results were obtained for a range of data acquisition times, namely 4, 6, 8, or 10 min, top to bottom, respectively. The scale bar indicates 2 mm. [Color figure can be viewed at wileyonlinelibrary.com]

TABLE III. Microvascularity levels calculated from *in vivo* SR-US images obtained following a bolus injection of MBs of different sizes, namely 1–2 μm, 3–4 μm, or 5–8 μm, and using a range of different US image acquisition times, i.e., 4, 6, 8, or 10 min.

	Microvascularity (% area)		
Time (min)	1–2 μm	3–4 μm	5–8 μm
4	6.5 ± 1.7	10.4 ± 1.4	10.3 ± 1.3
6	7.8 ± 1.4	12.9 ± 3.1	12.8 ± 1.1
8	8.6 ± 1.2	23.9 ± 3.4	24.4 ± 1.2
10	9.3 ± 1.4	25.7 ± 3.5	27.6 ± 2.1

microbubble contras agents (microbubble infusion rate 5 mL/h) showed that background tissue signal was well filtered while preserving the microbubble signal of interest. Thus, it confirmed that slow moving (close to stationary) MB signals were not removed along with the tissue signals.

In was observed that higher the background noise and tissue signal amplitude, more the number of singular values required to be eliminated for SVD filtration. Finding and eliminating higher number of singular values using a large DCE-US data, like ours, resulted in significantly higher processing time. In order to reduce the overall processing time of the SR-US algorithm, an empirically determined threshold value was used to eliminate low intensity background noise from the DCE-US image sequence prior to SVD filtering.

Accurate MB localization during SR-US image processing necessitates that they are spatially separated. Spatially close MBs can have overlapping point spread functions (PSFs), which can limit the precision of single MB localization. One way to overcome this challenge is to use hyper dilute MB concentrations. However, MB concentration within the microvascular network ultimately dictates their visualization in the SR-US image. Thus, for a fixed US imaging frame rate and image acquisition time, a reduced MB concentration means a reduced localization density and sparse spatial distribution. While the use of a high MB concentration yields a denser *in vivo* distribution, spatial inseparability of individual agents makes them less detectable. Thus, it is important to choose a suitable MB concentration, acquisition time, and US imaging rate when performing *in vivo* SR-US imaging.

Using a MB-sensitive harmonic imaging mode, our *in vivo* SR-US results obtained using size-selected MBs illustrates that larger contrast agent populations (3–4 μm and 5–8 μm) generate better results than smaller MB types (1–2 μm). Given the fundamental frequency of the transmitted US pulses, this result is consistent with the theoretical prediction as larger MBs are expected to oscillate more strongly leading to an enhanced US signal.[22] When comparing results obtained using smaller and larger MBs, the observed differences in SR-US image quality is attributed in part to the larger scattering cross-section (and thus the US backscattering) of the latter MB type.[5] In general, the number of MBs localized and counted to form a MB density map (i.e., SR-US

image) is fundamentally limited by the number of MBs that flow through a given blood vessel. In general, larger blood vessels (having a larger blood and MB volume) tend to have a higher super-resolved spatial distribution of MBs, whereas smaller vessels have a sparser spatial distribution. Notwithstanding, given the enhanced US signal from larger MBs (proportional to the square of the contrast agent radius), we hypothesize that SR-US imaging of larger microvascular structures may be compromised during the first few minutes after administering a bolus injection. During this initial phase when MB concentration and intravascular volume is high, detecting spatially separated MBs is problematic until clearance (dissolution) reaches a level that permits individual MB counting. Therefore, SR-US images of larger microvascular structures may exhibit a lower level of MB localizations (density) compared to the same vessels imaged using smaller MB types. It appears that the use of larger MB types improves visualization of smaller microvascular structures since these MBs are more easily detected and localized.

A moderate concentration of 2.5×10^7 MBs per injection appears to generate acceptable SR-US images. Increasing the concentration did not substantially improve skeletal muscle microvascular definition. Furthermore, the appearance of increased microvascularity may not be true since precise MB localization becomes compromised at higher MB concentrations. While using the size-selected MBs, an US imaging rate of at least 20 fps and image acquisition length of at least 8 min results in a generation of a SR-US image with depiction of sufficient microvascular detail. The necessary imaging time to reconstruct microvascular details, however, depends on the imaging frame rate used, the number of MB events detected on each image, and the density of vessels that needs to be reconstructed. The use of higher imaging frame rates or acquisition times does not appear to generate much more additional SR-US image features. However, higher frame rates are critically important for frame-to-frame MB tracking and velocity mapping.[16,20] Interestingly, larger sized MBs have a longer circulating half-life,[23] which means changing the acquisition time has a greater impact on SR-US imaging compared with the use of smaller MBs, which are cleared from the bloodstream rather quickly.

A limitation of the research presented is that we assumed that no motion occurred during neither US imaging of the hindlimb skeletal muscle tissue nor between repeat US imaging sessions. Future work will focus on implementation of motion correction techniques which will be important for SR-US imaging of organs or cancerous tissues. The introduction of real-time volumetric DCE-US imaging of MB contrast agents allows 4-dimensional (4D) data acquisition (3-dimensional space + time)[24–26] and the results presented herein will help guide the next-generation development of 4D SR-US imaging.

5. CONCLUSION

It was shown that MB size and concentration has a tremendous impact on SR-US image quality in addition to US system level consideration such as imaging rate and data acquisition length. All parameters should be carefully considered when using SR-US for any *in vivo* imaging application. Overall, SR-US was shown to be a powerful modality for visualizing microvascular features in skeletal muscle tissue and may represent a new tool for characterizing early functional changes such as associated with type 2 diabetes.

ACKNOWLEDGMENTS

This work was supported, in part, by funds provided by the Department of Bioengineering at the University of Texas at Dallas, NIH grants K25EB017222 and R21CA212851, and Texas CPRIT award RR150010.

[a]Author to whom correspondence should be addressed. Electronic mail: kenneth.hoyt@utdallas.edu.

REFERENCES

1. Dawson D, Vincent MA, Barrett EJ, et al. Vascular recruitment in skeletal muscle during exercise and hyperinsulinemia assessed by contrast ultrasound. *Am J Physiol Endocrinol Metab*. 2002;282:E714–E720.
2. Eckel RH, Kahn SE, Ferrannini E, et al. Obesity and type 2 diabetes: what can be unified and what needs to be individualized? *J Clin Endocrinol Metab*. 2011;96:1654–1663.
3. Tregaskiss AP, Goodwin AN, Bright LD, Ziegler CH, Acland RD. Three-dimensional CT angiography: a new technique for imaging microvascular anatomy. *Clin Anat*. 2007;20:116–123.
4. Nijenhuis RJ, Leiner T, Cornips EM, et al. Spinal cord feeding arteries at MR angiography for thoracoscopic spinal surgery: feasibility study and implications for surgical approach. *Radiology*. 2004; 233:541–547.
5. Szabo TL. *Diagnostic Ultrasound Imaging: Inside Out*, 2nd edn. Boston, MA: Academic Press; 2014.
6. Hoyt K, Umphrey H, Lockhart M, Robbin M, Forero-Torres A. Ultrasound imaging of breast tumor perfusion and neovascular morphology. *Ultrasound Med Biol*. 2015;41:2292–2302.
7. Saini R, Hoyt K. Recent developments in dynamic contrast-enhanced ultrasound imaging of tumor angiogenesis. *Imaging Med*. 2014;6:41–52.
8. Vincent MA, Clerk LH, Lindner JR, et al. Microvascular recruitment is an early insulin effect that regulates skeletal muscle glucose uptake in vivo. *Diabetes*. 2004;53:1418–1423.
9. Gessner RC, Frederick CB, Foster FS, Dayton PA. Acoustic angiography: a new imaging modality for assessing microvasculature architecture. *Int J Biomed Imaging*. 2013;2013:936593.
10. Gessner RC, Aylward SR, Dayton PA. Mapping microvasculature with acoustic angiography yields quantifiable differences between healthy and tumor-bearing tissue volumes in a rodent model. *Radiology*. 2012;264:733–740.
11. Viessmann OM, Eckersley RJ, Christensen-Jeffries K, Tang MX, Dunsby C. Acoustic super-resolution with ultrasound and microbubbles. *Phys Med Biol*. 2013;58:6447–6458.
12. Desailly Y, Pierre J, Couture O, Tanter M. Resolution limits of ultrafast ultrasound localization microscopy. *Phys Med Biol*. 2015;60:8723–8740.
13. O'Reilly MA, Hynynen K. A super-resolution ultrasound method for brain vascular mapping. *Med Phys*. 2013;40:110701.
14. Frinking PJ, Bouakaz A, Kirkhorn J, Ten Cate FJ, de Jong N. Ultrasound contrast imaging: current and new potential methods. *Ultrasound Med Biol*. 2000;26:965–975.
15. Demené C, Deffieux T, Pernot M, et al. Spatiotemporal clutter filtering of ultrafast ultrasound data highly increases Doppler and fultrasound sensitivity. *IEEE Trans Med Imaging*. 2015;34:2271–2285.
16. Errico C, Pierre J, Pezet S, et al. Ultrafast ultrasound localization microscopy for deep super-resolution vascular imaging. *Nature*. 2015;527:499–502.

17. Foiret J, Zhang H, Mahakian L, Tam S, Ferrara K. Super-localization of contrast agents in moving organs, first experiments in a rat kidney. *Proc IEEE Ultrasonics Sympos*; 2016, pp. 1–4.
18. Bar-Zion A, Tremblay-Darveau C, Solomon O, Adam D, Eldar Y. Fast vascular ultrasound imaging with enhanced spatial resolution and background rejection. *IEEE Trans Med Imaging*. 2016;36:169–180.
19. Lin F, Shelton SE, Espíndola D, Rojas JD, Pinton G, Dayton PA. 3-D ultrasound localization microscopy for identifying microvascular morphology features of tumor angiogenesis at a resolution beyond the diffraction limit of conventional ultrasound. *Theranostics*. 2017;7:196–204.
20. Christensen-Jeffries K, Browning RJ, Tang MX, Dunsby C, Eckersley RJ. In vivo acoustic super-resolution and super-resolved velocity mapping using microbubbles. *IEEE Trans Med Imaging*. 2015;34:433–440.
21. Sirsi S, Borden M. Microbubble compositions, properties and biomedical applications. *Bubble Sci Eng Technol*. 2009;1:3–17.
22. de Jong N, Hoff L, Skotland T, Bom N. Absorption and scatter of encapsulated gas filled microspheres: theoretical considerations and some measurements. *Ultrasonics*. 1992;30:95–103.
23. Sirsi S, Feshitan J, Kwan J, Homma S, Borden M. Effect of microbubble size on fundamental mode high frequency ultrasound imaging in mice. *Ultrasound Med Biol*. 2010;36:935–948.
24. Mahoney M, Sorace A, Warram J, Samuel S, Hoyt K. Volumetric contrast-enhanced ultrasound imaging of renal perfusion. *J Ultrasound Med*. 2014;33:1427–1437.
25. Hoyt K, Sorace A, Saini R. Quantitative mapping of tumor vascularity using volumetric contrast-enhanced ultrasound. *Invest Radiol*. 2012;47:167–174.
26. Hoyt K, Sorace A, Saini R. Volumetric contrast-enhanced ultrasound imaging to assess early response to apoptosis-inducing anti-death receptor 5 antibody therapy in a breast cancer animal model. *J Ultrasound Med*. 2012;31:1759–1766.